NANO EXPRESS   **Open Access**

CrossMark

Multiband and Broadband Absorption Enhancement of Monolayer Graphene at Optical Frequencies from Multiple Magnetic Dipole Resonances in Metamaterials

Bo Liu[1], Chaojun Tang[2*], Jing Chen[3,4,5*] , Ningyan Xie[3], Huang Tang[1], Xiaoqin Zhu[1] and Gun-sik Park[4]

Abstract

It is well known that a suspended monolayer graphene has a weak light absorption efficiency of about 2.3% at normal incidence, which is disadvantageous to some applications in optoelectronic devices. In this work, we will numerically study multiband and broadband absorption enhancement of monolayer graphene over the whole visible spectrum, due to multiple magnetic dipole resonances in metamaterials. The unit cell of the metamaterials is composed of a graphene monolayer sandwiched between four Ag nanodisks with different diameters and a SiO_2 spacer on an Ag substrate. The near-field plasmon hybridizations between individual Ag nanodisks and the Ag substrate form four independent magnetic dipole modes, which result into multiband absorption enhancement of monolayer graphene at optical frequencies. When the resonance wavelengths of the magnetic dipole modes are tuned to approach one another by changing the diameters of the Ag nanodisks, a broadband absorption enhancement can be achieved. The position of the absorption band in monolayer graphene can be also controlled by varying the thickness of the SiO_2 spacer or the distance between the Ag nanodisks. Our designed graphene light absorber may find some potential applications in optoelectronic devices, such as photodetectors.

Keywords: Light absorption, Monolayer graphene, Magnetic dipole resonances, Metamaterials, Plasmonics

Background

Graphene, a monolayer of carbon atoms tightly arranged in two-dimensional (2D) honeycomb lattice, was first separated from graphite experimentally in 2004 [1]. Since then, graphene has attracted enormous attentions in the scientific community, partly owing to its exceptional electronic and optical properties, including fast carrier velocity, tunable conductivity, and high optical transparency [2]. As one kind of 2D emerging materials, graphene has promising potentials in a wide variety of fields ranging from optoelectronics [3–6] to plasmonics [7–10], to metamaterials [11–15], etc. Due to its unique

conical band structure of Dirac fermions, the suspended and undoped graphene exhibits a universal absorption of approximately 2.3% within the visible and near-infrared regions, which is related to the fine structure constant in a monolayer atomic sheet [16, 17]. The optical absorption efficiency is impressive, considering that graphene is only about 0.34 nm thick. However, it is still too low to be useful for optoelectronic devices such as photodetectors and solar cells, which need considerably higher absorption values for efficient operation.

To overcome this problem, various physical mechanisms [18–43] to enhance absorption of graphene in the visible region have been proposed, which include strong photon localization on the defect layer in one-dimensional (1D) photonic crystals [18, 28, 33, 38], total internal reflection [19, 20, 23, 27], surface plasmon resonances [21, 22, 30, 31, 33], evanescent diffraction orders of the arrays of metal nanoparticles [34], and critical coupling to guided mode resonances [25, 26, 32, 34, 35, 37, 39–41]. Besides

* Correspondence: chaojuntang@126.com; jchen@njupt.edu.cn
[2]Center for Optics and Optoelectronics Research, Collaborative Innovation Center for Information Technology in Biological and Medical Physics, College of Science, Zhejiang University of Technology, Hangzhou 310023, China
[3]College of Electronic and Optical Engineering and College of Microelectronics, Nanjing University of Posts and Telecommunications, Nanjing 210023, China
Full list of author information is available at the end of the article

Liu *et al. Nanoscale Research Letters* (2018) 13:153

Page 2 of 7

the absorption enhancement in graphene, achieving multi-band and broadband light absorption in graphene is also important for some graphene-based optoelectronic devices from a practical point of view. But, it is still a challenge, as pointed out in the very recent reports [44–46]. At present, different approaches have been proposed to broaden the bandwidth of graphene absorption in wide frequency range from THz [44–62] and infrared [63–65] to optical frequencies [19, 23, 29, 31, 34–36, 38–40, 43]. Especially, a multi-resonator approach was proven to be a very effective method to resolve the bandwidth limitation of graphene absorption in the THz and infrared regions [45, 46, 62, 63]. In the multi-resonator approach, deep-subwavelength multiple resonators with different sizes are closely packed, which could extend the absorption bandwidth when their resonance frequencies overlap with each other. However, to the best of our knowledge, up to now there are only a few reports on such a multi-resonator approach to obtain multiband and broadband light absorption of graphene in the visible region.

In this work, by employing similar multi-resonator approach, we will numerically demonstrate multiband and broadband absorption enhancement of monolayer graphene in the whole visible wavelength range, which arise from a set of magnetic dipole resonances in metamaterials. The unit cell of metamaterials consists of a graphene monolayer sandwiched between four Ag nanodisks with different diameters and a SiO$_2$ spacer on an Ag substrate. The near-field plasmon hybridizations between individual Ag nanodisks and the Ag substrate form four independent magnetic dipole modes, which result into four-band absorption enhancement of monolayer graphene. When the magnetic dipole modes are tuned to be overlapped spectrally by changing the diameters of Ag nanodisks, a broadband absorption enhancement is achieved. The position of the absorption band in monolayer graphene can be also controlled by varying the thickness of the SiO$_2$ spacer or the distance between the Ag nanodisks.

Methods/Experimental

The designed metamaterials for multiband and broadband absorption enhancement of graphene at optical frequencies are schematically shown in Fig. 1. The unit cell of the metamaterials consists of a graphene monolayer sandwiched between four Ag nanodisks with different diameters and a SiO$_2$ spacer on an Ag substrate. We calculate the reflection and absorption spectra, and the distributions of electromagnetic fields by the commercial software package "EastFDTD, version 5.0," which is based on finite difference time domain (FDTD) method (www.eastfdtd.com). In our numerical calculations, the refractive index of SiO$_2$ is 1.45, and the frequency-dependent relative permittivity of Ag is taken from
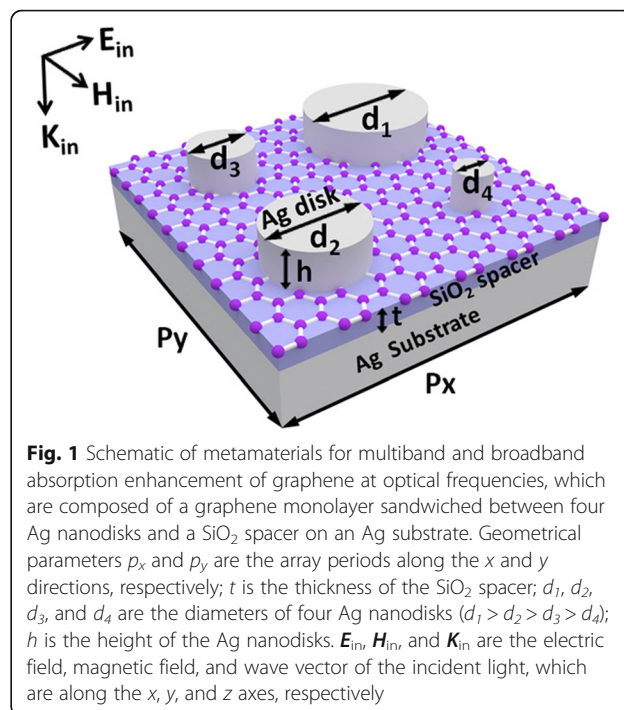

Fig. 1 Schematic of metamaterials for multiband and broadband absorption enhancement of graphene at optical frequencies, which are composed of a graphene monolayer sandwiched between four Ag nanodisks and a SiO$_2$ spacer on an Ag substrate. Geometrical parameters p_x and p_y are the array periods along the x and y directions, respectively; t is the thickness of the SiO$_2$ spacer; d_1, d_2, d_3, and d_4 are the diameters of four Ag nanodisks ($d_1 > d_2 > d_3 > d_4$); h is the height of the Ag nanodisks. $\boldsymbol{E}_{in}$, $\boldsymbol{H}_{in}$, and $\boldsymbol{K}_{in}$ are the electric field, magnetic field, and wave vector of the incident light, which are along the x, y, and z axes, respectively

experimental data [66]. Under the random-phase approximation, the complex surface conductivity σ of graphene is the sum of the intraband term σ_{intra} and the interband term σ_{inter} [67, 68], which are expressed as follows:

$$\sigma_{\text{intra}} = \frac{ie^2 k_B T}{\pi \hbar^2 (\omega + i/\tau)} \left(\frac{E_f}{k_B T} + 2 In \left(e^{-\frac{E_f}{k_B T}} + 1 \right) \right), \sigma_{\text{inter}}$$
$$= \frac{ie^2}{4\pi \hbar} In \left(\frac{2E_f - (\omega + i/\tau)\hbar}{2E_f + (\omega + i/\tau)\hbar} \right),$$
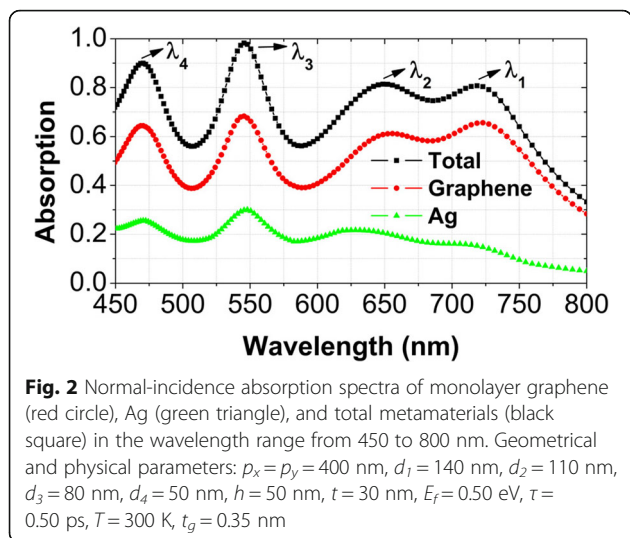
(1)

where ω is the frequency of incident light, e is electron charge, $\hbar$ is reduced Planck constant, E_f is Fermi energy (or chemical potential), τ is the relaxation time of electron-phonon, k_B is Boltzmann constant, T is temperature in K, and i is the imaginary unit. Graphene has an anisotropic relative permittivity tensor of ε_g expressed as

$$\varepsilon_g = \begin{pmatrix} 1 + i\sigma/(\omega\varepsilon_0 t_g) & 0 & 0 \\ 0 & 1 + i\sigma/(\omega\varepsilon_0 t_g) & 0 \\ 0 & 0 & 1 \end{pmatrix}, \quad (2)$$

where ε_0 is the permittivity of the vacuum, and t_g is the thickness of graphene sheet.

Results and Discussion
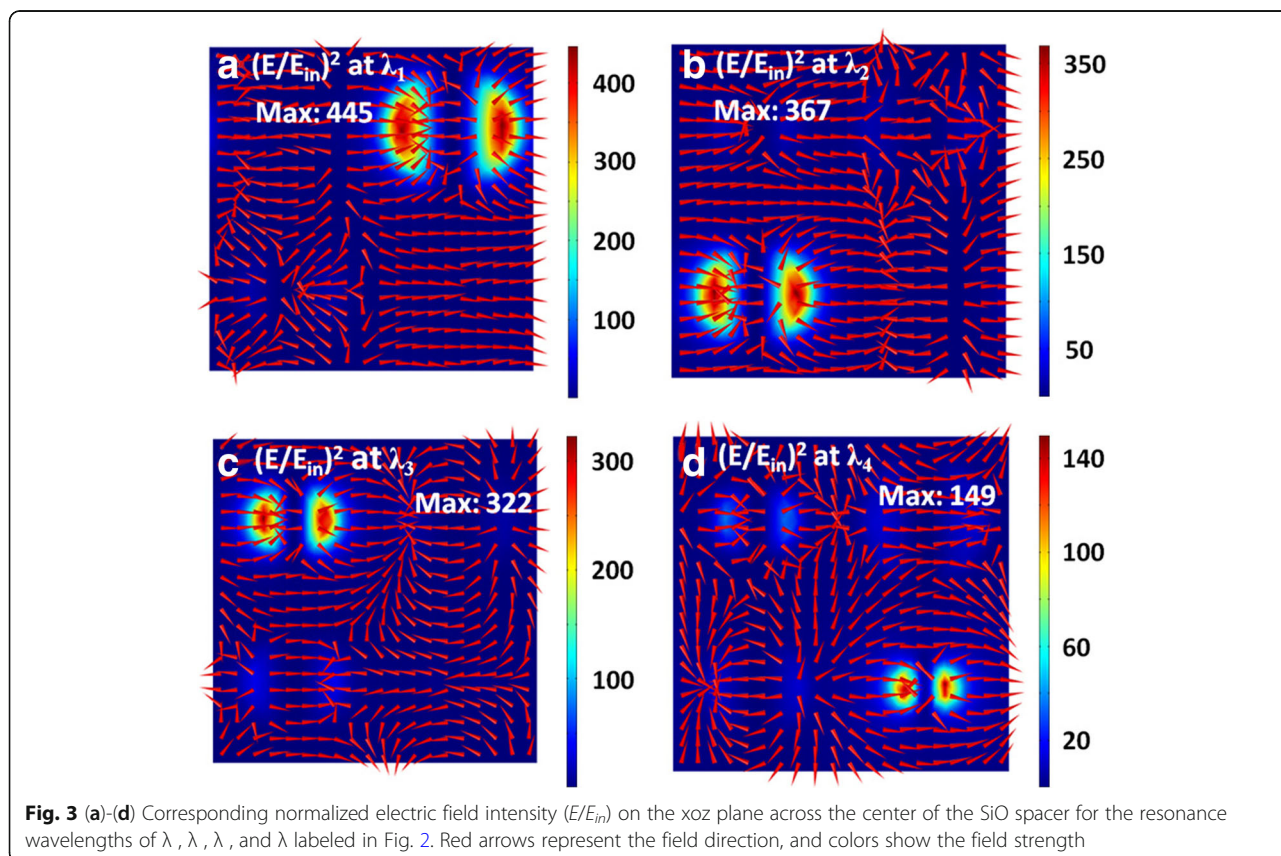
Figure 2 shows the calculated absorption spectra of graphene, Ag, and total metamaterials at normal incidence.

Liu *et al. Nanoscale Research Letters* (2018) 13:153

Page 3 of 7

Fig. 2 Normal-incidence absorption spectra of monolayer graphene (red circle), Ag (green triangle), and total metamaterials (black square) in the wavelength range from 450 to 800 nm. Geometrical and physical parameters: $p_x = p_y = 400$ nm, $d_1 = 140$ nm, $d_2 = 110$ nm, $d_3 = 80$ nm, $d_4 = 50$ nm, $h = 50$ nm, $t = 30$ nm, $E_f = 0.50$ eV, $\tau = 0.50$ ps, $T = 300$ K, $t_g = 0.35$ nm

One can clearly see four absorption peaks, whose resonance wavelengths are $\lambda_1 = 722.9$ nm, $\lambda_2 = 655.7$ nm, $\lambda_3 = 545.5$ nm, and $\lambda_4 = 468.8$ nm. At four absorption peaks, the light absorption in graphene can reach as high as 65.7, 61.2, 68.4, and 64.5%, respectively. Compared with a suspended monolayer graphene whose absorption efficiency is only 2.3% at optical frequencies [16, 17], the monolayer graphene in our designed metamaterials has an

absorption enhancement of more than 26 times. It is also clearly seen in Fig. 2 that the absorbed light is mainly dissipated in graphene rather than in Ag. Moreover, the total absorption at the third peak exceeds 98.5%, very similar to much reported metamaterial electromagnetic wave perfect absorbers [69–75], which have many potential applications such as solar cells [76–81].

To find the physical origins of above four absorption peaks, Figs. 3 and 4 plot the distributions of electric and magnetic fields at the resonance wavelengths of λ_1, λ_2, λ_3, and λ_4. At the resonance wavelength of λ_1, the electric fields are mainly concentrated near the left and right edges of the first Ag nanodisk with a diameter of d_1 (see Fig. 3a), and the magnetic fields are highly confined within the SiO$_2$ region under the first Ag nanodisk (see Fig. 4a). Such field distributions correspond to the excitation of a magnetic dipole mode [82–86], which steps from the near-field plasmon hybridization between the first Ag nanodisk and the Ag substrate. At the resonance wavelengths of λ_2, λ_3, and λ_4, the electromagnetic fields have the same distribution properties, but are localized in the vicinity of the second, third, and fourth Ag nanodisks with diameters of d_2, d_3, and d_4, respectively. In short, the excitations of four independent magnetic dipole modes lead to the appearance of four absorption peaks in Fig. 2.

Fig. 3 (**a**)-(**d**) Corresponding normalized electric field intensity (E/E_{in}) on the xoz plane across the center of the SiO spacer for the resonance wavelengths of λ , λ , λ , and λ labeled in Fig. 2. Red arrows represent the field direction, and colors show the field strength
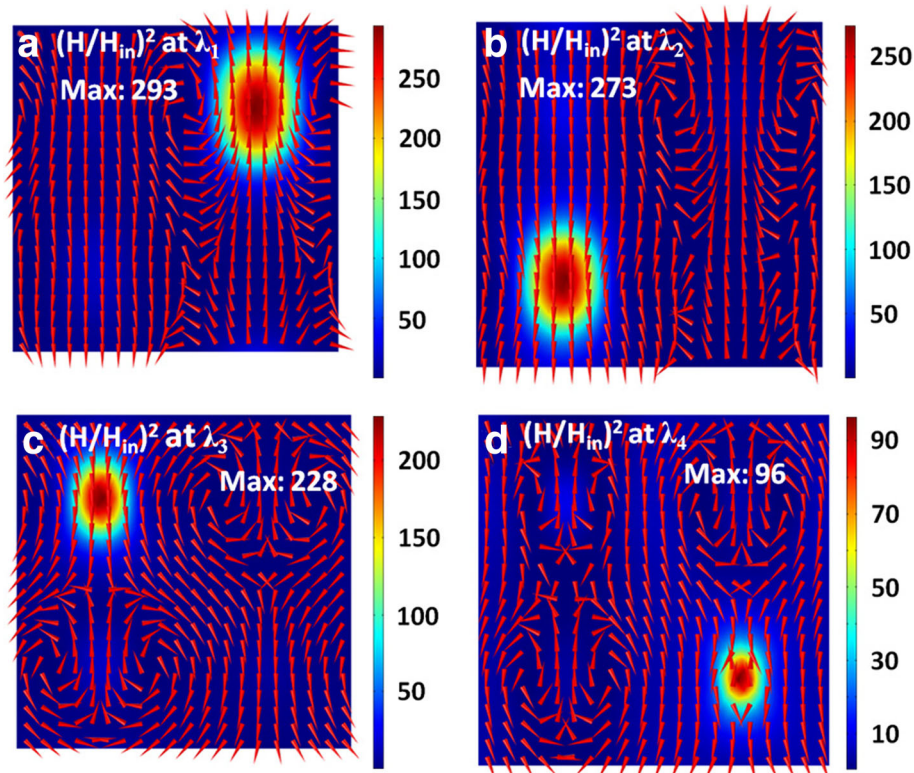
Fig. 4 The same as in Fig. 3, but for normalized magnetic field intensity $(H/H_{in})^2$

In our designed metamaterials, the near-field plasmon hybridizations between individual Ag nanodisks and the Ag substrate form four independent magnetic dipole modes, which result into multiband absorption enhancement of monolayer graphene in the visible wavelength range from 450 to 800 nm, with an average absorption efficiency exceeding 50% (please see Fig. 2). The resonance wavelength of each magnetic dipole mode can be conveniently tuned by changing the diameter of the corresponding Ag nanodisk. If the diameters of the Ag nanodisks are varied for the absorption peaks in Fig. 2 to approach one another, a broad high-absorption band of monolayer graphene will be formed. To demonstrate this, Fig. 5a presents the normal-incidence absorption spectra of monolayer graphene, when the diameters d_1, d_2, d_3, and d_4 of four Ag nanodisks are equal to 110, 90, 70, and 50 nm, respectively. In this case, a broadband absorption enhancement in the wavelength range from 450 to 650 nm is achieved by the spectral design on the overlapped absorption peaks, with the lowest (highest) absorption efficiency more than 50% (73%). For the diameters of the Ag nanodisks to be increased gradually, this broad high-absorption band is red-shifted, as shown in Fig. 5b, c.

Besides the diameters of the Ag nanodisks, we can tune the position of the absorption band in monolayer graphene by changing the thickness t of the SiO_2 spacer. Figure 6 shows the normal-incidence absorption spectra in monolayer graphene, for t to be increased from 25 to 45 nm. With the increasing t, the absorption band in monolayer
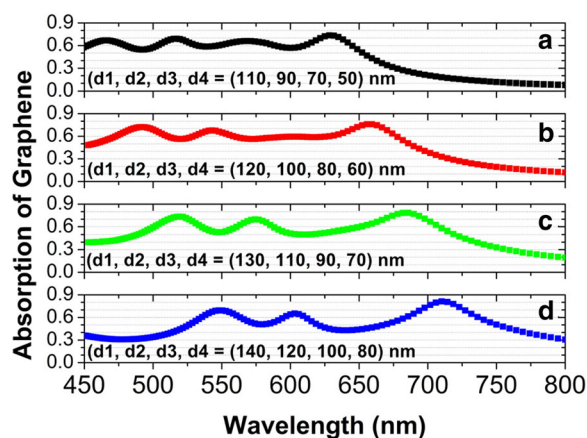

Fig. 5 (**a**)-(**d**) Corresponding normal-incidence absorption spectra of monolayer graphene in the wavelength range from 450 to 800 nm with the diameters of four Ag nanodisks are varied, but the other parameters are the same as those in Fig. 2
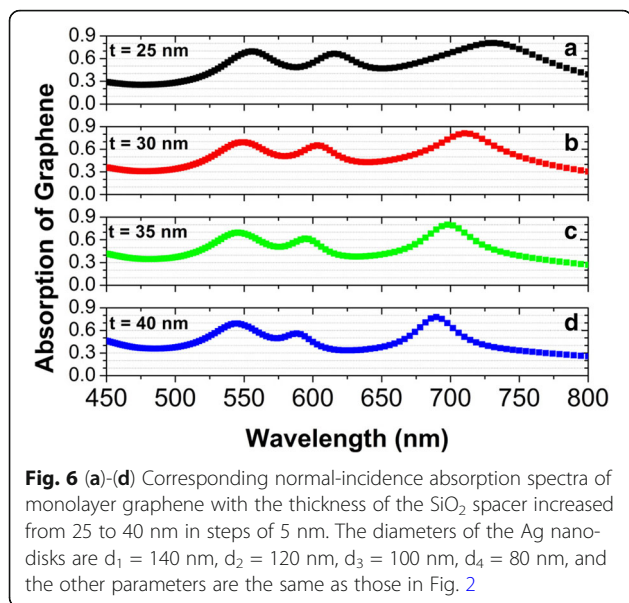
Liu et al. Nanoscale Research Letters (2018) 13:153

Page 5 of 7

Fig. 6 (a)-(d) Corresponding normal-incidence absorption spectra of monolayer graphene with the thickness of the SiO$_2$ spacer increased from 25 to 40 nm in steps of 5 nm. The diameters of the Ag nanodisks are d$_1$ = 140 nm, d$_2$ = 120 nm, d$_3$ = 100 nm, d$_4$ = 80 nm, and the other parameters are the same as those in Fig. 2

graphene will have an obvious blue-shift, because the near-field plasmon hybridizations between individual Ag nanodisks and the Ag substrate become weaker and thus magnetic dipole modes are blue-shifted [83].

In the above calculations, the coordinate points of four Ag nanodisks are ($\pm p_x$ /4, $\pm p_y$ /4), so the center distance l between the nearest-neighbor Ag nanodisks is 200 nm. By varying l, we can also tune the position of the absorption band in monolayer graphene. Figure 7 gives the normal-incidence absorption spectra in monolayer graphene, for l to be decreased from 220 to 160 nm. With the decreasing l, the absorption band in monolayer graphene is slightly blue-shifted, owing to the plasmon interactions among the Ag nanodisks.
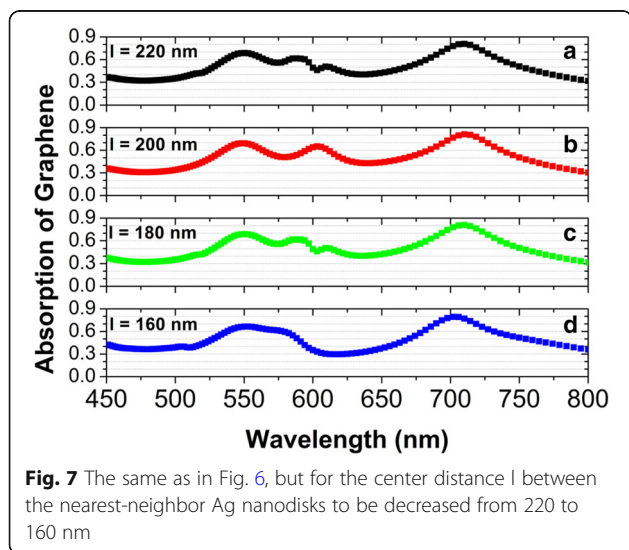

Fig. 7 The same as in Fig. 6, but for the center distance l between the nearest-neighbor Ag nanodisks to be decreased from 220 to 160 nm

Conclusions

In this work, we have numerically investigated multiband and broadband absorption enhancement of monolayer graphene at optical frequencies from multiple magnetic dipole resonances in metamaterials. The unit cell of the metamaterials consists of a graphene monolayer sandwiched between four Ag nanodisks with different diameters and a SiO$_2$ spacer on an Ag substrate. The near-field plasmon hybridizations between individual Ag nanodisks and the Ag substrate form four independent magnetic dipole modes, which result into multiband absorption enhancement of monolayer graphene in the visible wavelength range. When the magnetic dipole modes are tuned to be overlapped spectrally by changing the diameters of Ag nanodisks, a broadband absorption enhancement is achieved. The position of the absorption band in monolayer graphene can be also controlled, by varying the thickness of the SiO$_2$ spacer or the distance between the Ag nanodisks. The numerical results may have some potential applications in optoelectronic devices, such as photodetectors.

Availability of Data and Materials
All data are fully available without restriction.

Authors' Contributions
BL, CT, and JC contributed equally to this work. BL, CT, and JC performed the design, analyzed the data, and drafted the manuscript. CT, JC, and GP guided the idea and the simulations, and checked the figures. All authors read and approved the final manuscript.

Ethics Approval and Consent to Participate
We declare that there are no concerning data of human and animals.

Competing Interests
The authors declare that they have no competing interests.

Publisher's Note

Springer Nature remains neutral with regard to jurisdictional claims in published maps and institutional affiliations.

Author details
[1]School of Mathematics and Physics, Jiangsu University of Technology, Changzhou 213001, China. [2]Center for Optics and Optoelectronics Research, Collaborative Innovation Center for Information Technology in Biological and Medical Physics, College of Science, Zhejiang University of Technology, Hangzhou 310023, China. [3]College of Electronic and Optical Engineering and College of Microelectronics, Nanjing University of Posts and

Liu *et al. Nanoscale Research Letters* (2018) 13:153

Page 6 of 7

Telecommunications, Nanjing 210023, China. [4]Center for THz-driven Biological Systems, Department of Physics and Astronomy, Seoul National University, Seoul 151-747, South Korea. [5]State Key Laboratory of Millimeter Waves, Southeast University, Nanjing 210096, China.

References

1. Novoselov KS, Geim AK, Morozov SV, Firsov AA (2004) Electric field effect in atomically thin carbon films. Science 306:666–669
2. Ferrari AC et al (2015) Science and technology roadmap for graphene, related two-dimensional crystals, and hybrid systems. Nano 7:4598–4810
3. Ye Y, Dai L, Gan L, Meng H, Dai Y, Guo XF, Qin GG (2012) Novel optoelectronic devices based on single semiconductor nanowires (nanobelts). Nanoscale Res Lett 7:218
4. Lin F, Tong X, Wang YN, Bao JM, Wang ZMM (2015) Graphene oxide liquid crystals: synthesis, phase transition, rheological property, and applications in optoelectronics and display. Nanoscale Res Lett 10:435
5. Bao QL, Loh KP (2012) Graphene photonics, plasmonics, and broadband optoelectronic devices. ACS Nano 6:3677–3694
6. Koppens FHL, Mueller T, Avouris P, Ferrari AC, Vitiello MS, Polini M (2014) Photodetectors based on graphene, other two-dimensional materials and hybrid systems. Nat Nanotechnol 9:780–793
7. Koppens FHL, Chang DE, de Abajo FJG (2011) Graphene plasmonics: a platform for strong light-matter interactions. Nano Lett 11:3370–3377
8. Grigorenko AN, Polini M, Novoselov KS (2012) Graphene plasmonics. Nat Photonics 6:749–758
9. Low T, Avouris P (2014) Graphene plasmonics for terahertz to mid-infrared applications. ACS Nano 8:1086–1101
10. de Abajo FJG (2014) Graphene plasmonics: challenges and opportunities. ACS Photonics 1:135–152
11. Vakil A, Engheta N (2011) Transformation optics using graphene. Science 332:1291–1294
12. Chen PY, Alu A (2011) Atomically thin surface cloak using graphene monolayers. ACS Nano 5:5855–5863
13. Ju L, Geng BS, Horng J, Girit C, Martin M, Hao Z, Bechtel HA, Liang XG, Zettl A, Shen YR, Wang F (2011) Graphene plasmonics for tunable terahertz metamaterials. Nat Nanotechnol 6:630–634
14. Lee SH, Choi M, Kim TT, Lee S, Liu M, Yin X, Choi HK, Lee SS, Choi GG, Choi SY, Zhang X, Min B (2012) Switching terahertz waves with gate-controlled active graphene metamaterials. Nat Mater 11:936–941
15. Tassin P, Koschny T, Kafesaki M, Soukoulis CM (2012) A comparison of graphene, superconductors and metals as conductors for metamaterials and plasmonics. Nat Photonics 6:259–264
16. Nair RR, Blake P, Grigorenko AN, Novoselov KS, Booth TJ, Stauber T, Peres NMR, Geim AK (2008) Fine structure constant defines visual transparency of graphene. Science 320:1308
17. Dawlaty JM, Shivaraman S, Strait J, George P, Chandrashekhar M, Rana F, Spencer MG, Veksler D, Chen YQ (2008) Measurement of the optical absorption spectra of epitaxial graphene from terahertz to visible. Appl Phys Lett 93:131905
18. Liu JT, Liu NH, Li J, Li XJ, Huang JH (2012) Enhanced absorption of graphene with one-dimensional photonic crystal. Appl Phys Lett 101:052104
19. Pirruccio G, Moreno LM, Lozano G, Rivas JG (2013) Coherent and broadband enhanced optical absorption in graphene. ACS Nano 7:4810–4817
20. Ye Q, Wang J, Liu ZB, Deng ZC, Kong XT, Xing F, Chen XD, Zhou WY, Zhang CP, Tian JG (2013) Polarization-dependent optical absorption of graphene under total internal reflection. Appl Phys Lett 102:021912
21. Hashemi M, Farzad MH, Mortensen NA, Xiao SS (2013) Enhanced absorption of graphene in the visible region by use of plasmonic nanostructures. J Opt 15:055003
22. Zhu JF, Liu QH, Linc T (2013) Manipulating light absorption of graphene using plasmonic nanoparticles. Nano 5:7785–7789
23. Zhao WS, Shi KF, Lu ZL (2013) Greatly enhanced ultrabroadband light absorption by monolayer graphene. Opt Lett 38:4342–4345
24. Stauber T, Gómez-Santos G, de Abajo FJG (2014) Extraordinary absorption of decorated undoped graphene. Phys Rev Lett 112:077401
25. Grande M, Vincenti MA, Stomeo T, Bianco GV, de Ceglia D, Aközbek N, Petruzzelli V, Bruno G, De Vittorio M, Scalora M, D'Orazio A (2014) Graphene-based absorber exploiting guided mode resonances in one-dimensional gratings. Opt Express 22:31511–31519
26. Piper JR, Fan SH (2014) Total absorption in a graphene monolayer in the optical regime by critical coupling with a photonic crystal guided resonance. ACS Photonics 1:347–353
27. Dong B, Wang P, Liu ZB, Chen XD, Jiang WS, Xin W, Xing F, Tian JG (2014) Large tunable optical absorption of CVD graphene under total internal reflection by strain engineering. Nanotechnology 25:455707
28. Grande M, Vincenti MA, Stomeo T, de Ceglia D, Petruzzelli V, De Vittorio M, Scalora M, D'Orazio A (2014) Absorption and losses in one-dimensional photonic-crystal-based absorbers incorporating graphene. IEEE Photonics J 6:0600808
29. Miloua R, Kebbab Z, Chiker F, Khadraoui M, Sahraoui K, Bouzidi A, Medles M, Mathieu C, Benramdane N (2014) Peak, multi-peak and broadband absorption in graphene-based one-dimensional photonic crystal. Opt Commun 330:135–139
30. Cai YJ, Zhu JF, Liu QH (2015) Tunable enhanced optical absorption of graphene using plasmonic perfect absorbers. Appl Phys Lett 106:043105
31. Niu J, Luo M, Zhu JF, Liu QH (2015) Enhanced plasmonic light absorption engineering of graphene: simulation by boundary-integral spectral element method. Opt Express 23:4539–4551
32. Grande M, Vincenti MA, Stomeo T, Bianco GV, de Ceglia D, Aközbek N, Petruzzelli V, Bruno G, De Vittorio M, Scalora M, D'Orazio A (2015) Graphene-based perfect optical absorbers harnessing guided mode resonances. Opt Express 23:21032–21042
33. Deng XH, Liu JT, Yuan JR, Liao QH, Liu NH (2015) A new transfer matrix method to calculate the optical absorption of graphene at any position in stratified media. EPL 109:27002
34. Zheng GG, Zhang HJ, Xu YH, Liu YZ (2016) Enhanced absorption of graphene monolayer with a single-layer resonant grating at the Brewster angle in the visible range. Opt Lett 41:2274–2277
35. Long YB, Shen L, Xu HT, Deng HD, Li YX (2016) Achieving ultranarrow graphene perfect absorbers by exciting guided-mode resonance of one-dimensional photonic crystals. Sci Rep 6:32312
36. Lee YC, Lin KT, Chen HL (2016) Ultra-broadband and omnidirectional enhanced absorption of graphene in a simple nanocavity structure. Carbon 108:253–261
37. Long YB, Li YX, Shen L, Liang WY, Deng HD, Xu HT (2016) Dually guided-mode-resonant graphene perfect absorbers with narrow bandwidth for sensors. J Phys D Appl Phys 49:32LT01
38. Liu YJ, Xie X, Xie L, Yang ZK, Yang HW (2016) Dual-band absorption characteristics of one-dimensional photonic crystal with graphene-based defect. Optik 127:3945–3948
39. Zheng G, Cong JW, Chen YY, Xu LH, Xiao SR (2017) Angularly dense comb-like enhanced absorption of graphene monolayer with attenuated-total-reflection configuration. Opt Lett 42:2984–2987
40. Wang N, Bu LB, Chen YY, Zheng GG, Zou XJ, Xu LH, Wang JC (2017) Multiband enhanced absorption of monolayer graphene with attenuated total reflectance configuration and sensing application. Appl Phys Express 10:015102
41. Guo J, Wu LM, Dai XY, Xiang YJ, Fan DY (2017) Absorption enhancement and total absorption in a graphene-waveguide hybrid structure. AIP Adv 7:025101
42. Wan Y, Deng LG (2017) Modulation and enhancement of optical absorption of graphene-loaded plasmonic hybrid nanostructures in visible and near-infrared regions. J Appl Phys 121:163102
43. Huang FJ, Fu YQ (2017) Theoretical T circuit modeling of graphene-based metamaterial broadband absorber. Plasmonics 12:571–575
44. Amin M, Farhat M, Bagci H (2013) An ultra-broadband multilayered graphene absorber. Opt Express 21:29938–29948
45. Yi SY, Zhou M, Shi X, Gan QQ, Zi J, Yu ZF (2015) A multiple-resonator approach for broadband light absorption in a single layer of nanostructured graphene. Opt Express 23:10081–10090
46. Shi X, Ge LX, Wen XW, Han DH, Yang YP (2016) Broadband light absorption in graphene ribbons by canceling strong coupling at subwavelength scale. Opt Express 24:26357–26362
47. He SL, Chen T (2013) Broadband THz absorbers with graphene-based anisotropic metamaterial films. IEEE Trans Terahertz Sci Technol 3:757–763
48. Ning RX, Liu SB, Zhang HF, Bian BR, Kong XK (2014) A wide-angle broadband absorber in graphene-based hyperbolic metamaterials. Eur Phys J Appl Phys 68:20401

Liu *et al. Nanoscale Research Letters* (2018) 13:153

Page 7 of 7

49. Zhu ZH, Guo CC, Zhang JF, Liu K, Yuan XD, Qin SQ (2015) Broadband single-layered graphene absorber using periodic arrays of graphene ribbons with gradient width. Appl Phys Express 8:015102

50. Huang XJ, Zhang X, Hu ZR, Aqeeli M, Alburaikan A (2015) Design of broadband and tunable terahertz absorbers based on graphene metasurface: equivalent circuit model approach. IET Microw Antennas Propag 9:307–312

51. Khavasi A (2015) Design of ultra-broadband graphene absorber using circuit theory. J Opt Soc Am B 32:1941–1946

52. Gao RM, Xu ZC, Ding CF, Wu L, Yao JQ (2015) Graphene metamaterial for multiband and broadband terahertz absorber. Opt Commun 356:400–404

53. Wu PC, Papasimakis N, Tsai DP (2016) Self-affine graphene metasurfaces for tunable broadband absorption. Phys Rev Appl 6:044019

54. Yao G, Ling FR, Yue J, Luo CY, Luo Q, Yao JQ (2016) Dynamically electrically tunable broadband absorber based on graphene analog of electromagnetically induced transparency. IEEE Photonics J 8:7800808

55. Zhao YT, Wu B, Huang BJ, Cheng Q (2017) Switchable broadband terahertz absorber/reflector enabled by hybrid graphene-gold metasurface. Opt Express 25:7161–7169

56. Gao F, Zhu ZH, Xu W, Zhang JF, Guo CC, Liu K, Yuan XD, Qin SQ (2017) Broadband wave absorption in single-layered and nonstructured graphene based on far field interaction effect. Opt Express 25:9578–9586

57. Ye LF, Chen Y, Cai GX, Liu N, Zhu JF, Song ZY, Liu QH (2017) Broadband absorber with periodically sinusoidally-patterned graphene layer in terahertz range. Opt Express 25:11223–11232

58. Wang ZP, Hou YM (2017) Ultra-multiband absorption enhancement of graphene in a metal-dielectric-graphene sandwich structure covering terahertz to mid-infrared regime. Opt Express 25:19185–19194

59. Zhang Y, Shi Y, Liang CH (2017) Broadband tunable graphene-based metamaterial absorber. Opt Mater Express 6:3036–3044

60. Arik K, AbdollahRamezani S, Khavasi A (2017) Polarization insensitive and broadband terahertz absorber using graphene disks. Plasmonics 12:393–398

61. Xiao BG, Gu MY, Xiao SS (2017) Broadband, wide-angle and tunable terahertz absorber based on cross-shaped graphene arrays. Appl Opt 56: 5458–5462

62. Zhang YP, Li Y, Cao YY, Liu YZ, Zhang HY (2017) Graphene induced tunable and polarization-insensitive broadband metamaterial absorber. Opt Commun 382:281–287

63. Deng BC, Guo QS, Li C, Wang HZ, Ling X, Farmer DB, Han SJ, Kong J, Xia FN (2016) Coupling-enhanced broadband mid-infrared light absorption in graphene plasmonic nanostructures. ACS Nano 10:11172–11178

64. Xia SX, Zhai X, Huang Y, Liu JQ, Wang LL, Wen SC (2017) Multi-band perfect plasmonic absorptions using rectangular graphene gratings. Opt Lett 42: 3052–19194

65. Ying XX, Pu Y, Luo Y, Peng H, Li Z, Jiang YD, Xu J, Liu ZJ (2017) Enhanced universal absorption of graphene in a Salisbury screen. J Appl Phys 121: 023110

66. Johnson PB, Christy RW (1972) Optical constants of the noble metals. Phys Rev B 6: 4370-4379

67. Zhu BF, Ren GB, Zheng SW, Lin Z, Jian SS (2013) Nanoscale dielectric-graphene-dielectric tunable infrared waveguide with ultrahigh refractive indices. Opt Express 21:17089–17096

68. Xiang YJ, Guo J, Dai XY, Wen SC, Tang DY (2014) Engineered surface Bloch waves in graphene-based hyperbolic metamaterials. Opt Express 22:3054–3062

69. Watts CM, Liu XL, Padilla WJ (2012) Metamaterial electromagnetic wave absorbers. Adv Mater 24:OP98–OP120

70. Cui YX, He YR, Jin Y, Ding F, Yang L, Ye YQ, Zhong SM, Lin YY, He SL (2014) Plasmonic and metamaterial structures as electromagnetic absorbers. Laser Photonics Rev 8:495–520

71. Ra'di Y, Simovski CR, Tretyakov SA (2015) Thin perfect absorbers for electromagnetic waves: theory, design, and realizations. Phys Rev Appl 3:037001

72. Wang PW, Chen NB, Tang CJ, Chen J, Liu FX, Sheng SQ, Yan B, Sui CH (2017) Engineering the complex-valued constitutive parameters of metamaterials for perfect absorption. Nanoscale Res Lett 12:276

73. Liu ZQ, Liu GQ, Fu GL, Liu XS, Wang Y (2016) Multi-band light perfect absorption by a metal layer-coupled dielectric metamaterial. Opt Express 24: 5020–5025

74. Liu ZQ, Liu XS, Huang S, Pan PP, Chen J, Liu GQ, Gu G (2015) Automatically acquired broadband plasmonic-metamaterial black absorber during the metallic film-formation. ACS Appl Mater Interfaces 7(8):4962–4968

75. Liu XS, Chen J, Liu JS, Huang ZP, Yu MD, Pan PP, Liu ZQ (2017) III-V semiconductor resonators: a new strategy for broadband light perfect absorbers. Appl Phys Express 10(11):111201

76. Wang Y, Zhou L, Zheng QH, Lu H, Gan QG, Yu ZF, Zhu J (2017) Spectrally selective solar absorber with sharp and temperature dependent cut-off based on semiconductor nanowire arrays. Appl Phys Lett 110(20):201108

77. Zhou L, Zhuang SD, He CY, Tan YL, Wang ZL, Zhu J (2017) Self-assembled spectrum selective plasmonic absorbers with tunable bandwidth for solar energy conversion. Nano Energy 32:195–200

78. Tang MY, Zhou L, Gu S, Zhu WD, Wang Y, Xu J, Deng ZT, Yu T, Lu ZD, Zhu J (2016) Fine-tuning the metallic core-shell nanostructures for plasmonic perovskite solar cells. Appl Phys Lett 109(18):183901

79. Zhou L, Tan YL, Wang JY, Xu WC, Yuan Y, Cai WS, Zhu SN, Zhu J (2016) 3D self-assembly of aluminium nanoparticles for plasmon-enhanced solar desalination. Nat Photonics 10(6):393–398

80. Zhou L, Tan YL, Ji DX, Zhu B, Zhang P, Xu J, Gan QQ, Yu ZF, Zhu J (2016) Self-assembly of highly efficient, broadband plasmonic absorbers for solar steam generation. Sci Adv 2:e1501227

81. Zhou L, Yu XQ, Zhu J (2014) Metal-core/semiconductor-shell nanocones for broadband solar absorption enhancement. Nano Lett 14(2):1093–1098

82. Liu B, Tang CJ, Chen J, Yan ZD, Zhu MW, Sui YX, Tang H (2017) The coupling effects of surface plasmon polaritons and magnetic dipole resonances in metamaterials. Nanoscale Res Lett 12:586

83. Hao J, Wang J, Liu X, Padilla WJ, Zhou L, Qiu M (2010) High performance optical absorber based on a plasmonic metamaterial. Appl Phys Lett 96: 251104

84. Song ZY, Zhang BL (2014) Wide-angle polarization-insensitive transparency of a continuous opaque metal film for nearinfrared light. Opt Express 22: 6519–6525

85. Tang CJ, Yan ZD, Wang QG, Chen J, Zhu MW, Liu B, Liu FX, Sui CH (2015) Ultrathin amorphous silicon thin-film solar cells by magnetic plasmonic metamaterial absorbers. RSC Adv 5:81866–81874

86. Tang CJ, Yan B, Wang QG, Chen J, Yan ZD, Liu FX, Chen NB, Sui CH (2017) Toroidal dipolar excitation in metamaterials consisting of metal nanodisks and a dielectric spacer on metal substrate. Sci Rep 7:582